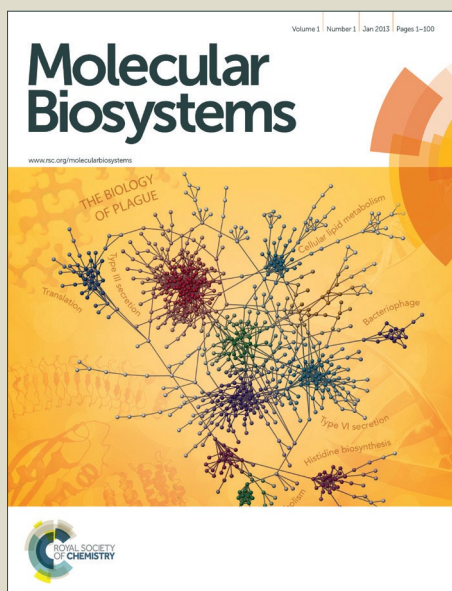


Molecular BioSystems

Accepted Manuscript



This is an *Accepted Manuscript*, which has been through the Royal Society of Chemistry peer review process and has been accepted for publication.

Accepted Manuscripts are published online shortly after acceptance, before technical editing, formatting and proof reading. Using this free service, authors can make their results available to the community, in citable form, before we publish the edited article. We will replace this *Accepted Manuscript* with the edited and formatted *Advance Article* as soon as it is available.

You can find more information about *Accepted Manuscripts* in the [Information for Authors](#).

Please note that technical editing may introduce minor changes to the text and/or graphics, which may alter content. The journal's standard [Terms & Conditions](#) and the [Ethical guidelines](#) still apply. In no event shall the Royal Society of Chemistry be held responsible for any errors or omissions in this *Accepted Manuscript* or any consequences arising from the use of any information it contains.



www.rsc.org/molecularbiosystems

Furanodiene alters mitochondrial function in doxorubicin-resistant MCF-7 human breast cancer cells in an AMPK-dependent manner

Zhang-Feng Zhong^{1,*}, Wen Tan^{2,*}, William W. Qiang^{1,3,*}, Virginia L. Scofield⁴, Chun-Ming Wang¹, Wen-An Qiang^{5,#}, Yi-Tao Wang^{1,#}

1. Institute of Chinese Medical Sciences, State Key Laboratory of Quality Research in Chinese Medicine, University of Macau, Macao 999078, China

2. School of Pharmacy, Lanzhou University, Lanzhou, Gansu province 730000, China

3. Yale University, New Haven, Connecticut 06511, USA

4. Department of Microbiology and Immunology, University of Texas Health Science Center at San Antonio, Edinburg, Texas 78541, USA

5. Division of Reproductive Science in Medicine, Department of Obstetrics and Gynecology, Feinberg School of Medicine at Northwestern University, Chicago, Illinois 60611, USA

*The authors contributed equally to this work.

#Corresponding authors:

Prof. Yi-Tao Wang

Institute of Chinese Medical Sciences, University of Macau,

Avenida da Universidade, Taipa, Macao, China

E-mail: ytwang@umac.mo

Dr. Wen-An Qiang

Department of Obstetrics and Gynecology, Feinberg School of Medicine at Northwestern University, 303 East Superior Street, Lurie 7-250, Chicago, Illinois 60611, United States of America

E-mail: W-qiang@northwestern.edu

Abstract

Furanodiene is a bioactive sesquiterpene isolated from the spice-producing *Curcuma wenyujin* plant (Y.H.Chen et C.Ling) (*C. wenyujin*), which is a commonly prescribed herb used in clinical cancer therapy by modern practitioners of traditional Chinese medicine. Previously, we have shown that furanodiene inhibits breast cancer cell growth both *in vitro* and *in vivo*, however, the mechanism for this effect is not yet known. In this study, therefore, we asked (1) whether cultured breast cancer cells made resistant to chemotherapeutic agent doxorubicin (DOX) via serial selection protocols are susceptible to furanodiene's anticancer effect, and (2) whether AMP-activated protein kinase (AMPK), which is a regulator of cellular energy homeostasis in eukaryotic cells, participates in this effect.

We show here (1) that doxorubicin-resistant MCF-7 (MCF-7/DOX^R) cells treated

with furanodiene exhibit altered mitochondrial function and reduced levels of ATP content, resulting in apoptotic cell death, and (2) that AMPK is central to this effect. In these cells, furanodiene (as opposed to doxorubicin) noticeably affects the phosphorylation of AMPK and AMPK pathway intermediates, ACLY and GSK-3 β , suggesting that furanodiene reduces mitochondrial function and cellular ATP levels by way of AMPK activation. Finally, we find that the cell permeable agent and AMPK inhibitor compound C (CC), abolishes furanodiene-induced anticancer activity in these MCF-7/DOX^R cells, with regards to cell growth inhibition and AMPK activation; in contrast, AICAR (5-aminoimidazole-4-carboxamide-1- β -4-ribofuranoside, acadesine), an AMPK activator, augments furanodiene-induced anticancer activity. Furthermore, specific knockdown of AMPK in MCF-7/DOX^R cells protects these cells from furanodiene-induced cell death.

Taken together, these findings suggest that AMPK and its pathway intermediates are promising therapeutic targets for treating chemoresistant breast cancer, and that furanodiene may be an important chemical agent incorporated in next-generation chemotherapy protocols.

Key words

furanodiene; mitochondrial function; AMPK; chemoresistance; metabolic

reprogramming

Highlights

- This is the first study reporting that furanodiene exhibits anticancer effects on doxorubicin-induced chemoresistant tumor cells.
- This is the first study reporting that furanodiene alters mitochondrial function in an AMPK-dependent manner.
- The AMPK-mediated effects of furanodiene, documented here, suggest that doxorubicin-induced chemoresistance can be abolished, by furanodiene or other compounds that activate AMPK, in breast cancer cells.

1. Introduction

Breast cancer is the most frequently diagnosed tumor type in women worldwide. Despite advances in our understanding to better prevent, diagnose, and treat the disease, breast cancer still represents a major cause of mortality as standard treatment options, including surgical excision of tumor tissue and chemotherapy, have yet to adapt to the development of multidrug resistance (MDR). This therapeutic mismatch commonly results in chemotherapy failure, tumor recurrence and further progression, leading to outcomes with low prognosis¹.

Cancer cells are metabolically distinct from normal cells upon transformation. The new metabolic signature is commonly referred to as the ‘Warburg Effect,’ which

is characterized by enhanced glycolysis and reduced mitochondrial oxidation². Other changes associated with the Warburg Effect include the increased expression and activity of ATP-binding cassette transporters (ABC transporters), which has been shown to contribute to drug efflux and promote chemoresistance^{3, 4}, and downregulated AMP-activated kinase (AMPK) activity, an adaptive response to promote tumor cell survival under the Warburg conditions of increased glycolysis, and decreased mitochondrial ATP production⁵. While the molecular mechanisms of MDR onset are still unclear, there is evidence that (1) treatment with chemotherapeutic drugs increases the expression of several ABC transporters associated with MDR⁶, and that (2) across many different MDR cell-lines, including MCF-7, MDR cells clearly overexpressed ABC transporter genes in comparison with their drug-sensitive parental lines⁷. This suggests that global metabolic changes in cancer, such as those mediated by the Warburg Effect, maybe potentially influence the development of MDR, and can be investigated to identify promising therapeutic targets for treating chemoresistant breast cancer.

AMP-activated protein kinase (AMPK), an energy sensor presents in healthy eukaryotic cells, is also an important enzymatic control of energy homeostasis during cancer cell transformation and proliferation⁸. This enzyme is activated by intracellular conditions that increase AMP to ATP and ADP to ATP ratios⁹, and thus is sensitive to metabolic stresses, such as hypoxia and glucose starvation, wherein the precipitated redox dysregulation and mitochondrial dysfunction can cause abnormal ATP consumption and suppress mitochondrial ATP synthesis, leading to AMPK activation. AMPK activation inhibits anabolic metabolism, including gluconeogenesis and fatty acid synthesis, and stimulates catabolic metabolism, including fatty acid oxidation¹⁰⁻¹³, while enhancing mitochondrial oxidation and biogenesis to exert anti-Warburg and

anti-proliferative effects in lymphomas¹⁴. Therefore, AMPK performs a central role in regulating cell metabolism.

As noted above, AMPK activation is a normal compensatory response to anabolic metabolism inhibition, wherein ATP-consuming processes are switched off. Paradoxically, cancer cells, toward promoting their adaptation to metabolic stresses, hijack AMPK activation. This counterintuitive, controversial role of AMPK has been studied and discussed in detail¹⁵, and we now know that AMPK plays many roles in tumor initiation, growth and spread. For example, AMPK-dependent autophagy of pancreatic cancer cells, leading to cell death, can be induced by cannabinoid treatment¹⁶. As noted above, AMPK has been shown to maintain nicotinamide adenine dinucleotide phosphate (NADPH) levels, exploiting the Warburg Effect in favor of tumor cell survival under energy stress¹⁷. Loss of AMPK signaling contributes to the Warburg Effect in H1299 non-small-cell lung tumor cells and HCT116 colon cancer cells, and it also supports tumor growth *in vivo*¹⁴. In kidney tumor cells grown under fumarate hydrate (FH) deficiency, AMPK-assisted p53 and hypoxia-inducible factor 1 α (HIF-1 α) promote the Warburg Effect, contributing to tumor growth¹⁸. In C4-2 prostate cancer cells, knockdown of AMPK by α 1 shRNA promotes cell proliferation and maintains the malignant phenotype *in vitro*¹⁹.

Agents that activate AMPK, such as OSU-53, are under investigation as a therapy for triple-negative breast cancer²⁰. The antidiabetic drug metformin has also been examined for its anticancer properties, which include re-sensitizing acquired MDR MCF-7/5-FU and innate MDR MDA-MB-231 breast cancer cells to chemotherapeutics²¹. This suggests that other activators of AMPK may have similar anticancer effects.

Furanodiene is a bioactive sesquiterpene found abundantly in *Curcuma wenyujin*

(Y.H.Chen et C.Ling), a Chinese herb possessing anticancer properties. *Curcuma wenyujin* is widely prescribed for clinical cancer therapy by modern practitioners of traditional Chinese medicine, and compounds isolated from *C. wenyujin* have been approved by the State Food and Drug Administration (SFDA) as new second-class drugs for cancer chemotherapy^{22, 23}. Furanodiene, one of these isolates, exhibits a variety of pharmacological properties, which include hepatoprotection, anti-inflammation, anti-angiogenesis and anticancer effects, and its anti-proliferative and pro-apoptotic effects have been studied in a variety of cancer cell lines (HepG2, HL-60, HeLa, PC3, SGC-7901, HT-1080, MCF-7, MDA-MB-231, A549, NIH-H1299, 95-D)²⁴⁻³⁰. Work in our laboratory has shown that furanodiene inhibits the growth of breast cancer cells *in vitro* and *in vivo*²³, and that it enhances tamoxifen-induced growth inhibition, in estrogen receptor alpha- (ER α -) positive breast cancer cells, in a peroxisome proliferator-activated receptor γ (PPAR γ) independent manner³¹. Work by others has shown that furanodiene suppresses migration and invasion of metastatic breast cancer cells *in vitro*³². In this study, therefore, we sought to identify mechanisms underlying the effects of furanodiene on doxorubicin-induced chemoresistant breast cancer MCF-7 cells. We hypothesized that AMPK activation is involved in furanodiene-induced anticancer effects.

2. Materials and Methods

2.1. Reagents and Cell Culture

Furanodiene was purchased from the National Institutes for Food and Drug Control

(Beijing, China). Doxorubicin (DOX) was obtained from Sigma-Aldrich (St. Louis, USA). RPMI-1640 culture medium was purchased from Gibco (Maryland, USA). Fetal bovine serum (FBS), phosphate-buffered saline (PBS), penicillin-streptomycin (PS), and 0.25% (w/v) trypsin/1 mM EDTA were obtained from Invitrogen (Carlsbad, USA). 3-[4, 5-Dimethyl-2-thiazolyl]-2, 5-diphenyltetrazolium bromide (MTT), MitoTracker® Deep Red FM, propidium iodide (PI), and Annexin V/PI detection kits were obtained from Molecular Probes (Eugene, USA). Radioimmunoprecipitation assay (RIPA) lysis buffer was obtained from Beyotime (Shanghai, China). The ATP colorimetric/fluorometric assay kit was obtained from Biovision (California, USA). Primary antibodies against phosphor-ATP-Citrate Lyase (p-ACLY) (Ser455), ATP-Citrate Lyase (ACLY), p-GSK-3 β (Ser9), AMPK α , p-AMPK α (Thr172), HER2, β -actin, and GAPDH, and the appropriate secondary antibodies, were purchased from Cell Signaling (Danvers, USA).

The MCF-7 human breast cancer cell line was purchased from American Type Culture Collection (USA). To induce doxorubicin resistance, these cells were cultured with RPMI1640 medium containing fetal bovine serum (10%), penicillin (100 units/mL), and streptomycin (100 μ g/mL), at 37°C in a humidified atmosphere of 5% CO₂ in air. Doxorubicin-resistance was established by stepwise exposure to increased concentrations of doxorubicin, as described previously³³.

2.2. Mitochondrial Function Assay

Cells were seeded in 6-well plates at a density of 2×10^5 /well, and allowed to adhere overnight. Then, a 24-hour serum-free starvation was carried out to synchronize the cell division in the cultures. Cells were treated with furanodiene (0, 50, 100 μ M) or doxorubicin (2 μ M) for four hours, and then harvested, washed with PBS, and re-suspended gently in serum-free RPMI 1640 medium with MitoTracker[®] Deep Red probe (100 nM). Cells were protected from light, and exposed to the probe for 15 minutes at room temperature. Then, cells were refreshed with pre-warmed medium and analyzed by flow cytometry (BD FACS Canto[™], BD Biosciences, San Jose, USA).

2.3. ATP Production Assay

Cells were seeded in 60-mm Petri dishes at a density of 5×10^5 /dish, allowed to adhere overnight, and then treated with furanodiene (0, 50, 100 μ M) or doxorubicin (2 μ M) for four hours. The cells were then lysed with assay buffer and prepared according to the manufacturer's instructions using 500 μ g loading protein. Fluorescence (Ex/Em 535/587 nm) was measured using a SpectraMax M5 microplate reader (Molecular Devices). Fluorescence was expressed as a percentage of the values in control untreated cells.

2.4. Cell Growth and Cell Density Assay

Cell number images were captured with a microscope (Olympus MVX10, Japan) equipped with a digital camera (ColorView II, Soft Imaging System, Olympus) after the indicated drug treatments, and cell numbers were quantitated under a 100× magnification. Representative cell counts were based on at least three independent experiments.

2.5. Cell Viability Assay

MCF-7 cell viability was measured by the MTT assay³⁴. The cells were seeded in 96-well plates at density of 1×10^4 /well, and allowed to adhere overnight. Then, a 24-hour serum-free starvation was carried out to synchronize cell division in the cultures, before drug treatment with either doxorubicin or furanodiene for another 24 hours. When these cells are lysed, viable cells form formazan, which can be measured spectrophotometrically at 570 nm. To the formazan measurement, we used a SpectraMax M5 microplate reader (Molecular Devices). Cell viability was expressed as a percentage of formazan absorbance relative to the formazan absorbance in untreated control cells.

2.6. Cell Cycle and Apoptosis Assay

Cell cycle distributions were determined as previously described³². In brief, after furanodiene treatment (100 μ M) for 24 hours, cells were harvested via centrifugation, washed with ice-cold PBS, re-suspended in 70% (v/v) ice-cold ethanol for fixation, and then kept at -20°C overnight. The fixed cells were then incubated with a propidium iodide (PI) staining solution (20 μ g/mL PI, 8 μ g/mL RNase), for 30 minutes in the dark. Apoptosis induced by furanodiene, in doxorubicin-resistant MCF-7 (MCF-7/DOX^R) cells, was determined by Annexin V/PI labeling according to the manufacturer's protocol (Invitrogen). Cell cycle distribution and apoptosis were determined by flow cytometry (BD FACS CantoTM, BD Biosciences, San Jose, USA), based on DNA content in the cells and the sub-G₁ cell population, respectively. The data were analyzed using Mod Fit LT software (version 3.0).

2.7. Western Blotting

For Western blotting, the cells were seeded in 25-cm² flasks at a density of 1×10⁶/flask. After cell adhesion, drug treatment was carried out for 24 hours, as described above. Cell lysates were prepared and centrifuged for 20 minutes at 4°C, after which the total protein content was determined using a BCA protein assay reagent kit. Equal amounts of total protein were loaded into the wells of SDS-PAGE

(8%) gels and subjected to electrophoresis, after which the gels were transferred to methanol-activated PVDF membranes. After a 1-hour blocking incubation in non-fat milk (5%), the membranes were incubated first for two hours in primary antibodies (1:1000 dilution), followed by a 1-hour incubation in the secondary antibodies (1:1000 dilution), at room temperature. Immunoreactive bands were visualized and quantitated using an Enhanced Chemiluminescence (ECL) Western blotting detection kit (Amersham). Band densitometry was normalized by either β -actin or GAPDH, which were used as the loading controls.

2.8. Transfection and shRNA

Transfection with plasmids was performed as described previously³⁵. The AMPK

shRNA sequence was

5'-GATGATGTCAGATGGTGAATTTAAGTTCTCTAAATTCACCATCTGACATCA
TTT-3'. The target sequence

5'-GTTCTCCGAACGTGTCACGTTTCAAGAGAACGTGACACGTTCCGAGAAT
T-3' was used as a non-silencing control. Doxorubicin-resistant cells were transfected with shRNAs using Lipofectamine 2000, according to the manufacturer's instructions (Invitrogen, Carlsbad, CA, USA). After four hours of transfection, the cells were first refreshed and then cultured in complete medium containing 10% fetal bovine serum, 100 units/mL penicillin, and 100 μ g/mL streptomycin in 6-well plates, for a further 48

hours, before furanodiene treatment, which was conducted as described above.

2.9. Statistical Analysis

All data are expressed as the mean of at least three separately performed experiments, plus or minus standard deviation. The significance of the differences was evaluated by GraphPad Prism software (GraphPad Software, USA). Newman-Keuls multiple comparison tests were performed for *post hoc* pairwise comparisons. *p*-values less than 0.05 were considered as significance.

3. Results

3.1. Furanodiene suppresses mitochondrial function in doxorubicin-resistant MCF-7 (MCF-7/DOX^R) human breast cancer cells.

To assess the effect of furanodiene on mitochondrial function in MCF-7/DOX^R cells, these cells were treated with furanodiene in increased doses (0, 50, 100 μ M) or with doxorubicin (2 μ M) for four hours. Flow cytometry analysis using MitoTracker[®] Deep Red probe (100 nM) detected and quantitated differences in mitochondrial function between control and treated cells, as shown in **Fig. 1A**, and differences in mean fluorescence intensity (MFI) were assessed after normalizing treatment

intensities to the untreated control, as shown in **Fig. 1B**. Mitochondrial functions of doxorubicin-treated MCF-7/DOX^R cells are not significantly different from those of untreated control MCF-7/DOX^R cells, as reflected by similar MitoTracker® Deep Red MFIs (**Figs. 1A, 1B**). This finding confirms that serial selection of cultured MCF-7 cells resistant to doxorubicin-induced apoptosis indeed produces MCF-7/DOX^R cells, at least with respect to mitochondrial function. These data also show that furanodiene treatment significantly suppresses mitochondrial function, in a dose-dependent fashion. Moreover, treatment with doxorubicin in these cultured MCF-7/DOX^R cells does not significantly affect cellular ATP content (measured using an ATP kit), further confirming doxorubicin-resistance. In addition to its effect on mitochondrial function, documented above, furanodiene treatment (for 24 hours at 50 or 100 μ M) significantly suppresses ATP content in treated cells, in a dose-dependent manner, as shown in **Fig. 1C**.

3.2. Furanodiene regulates phosphorylation of AMPK pathway signaling intermediates in MCF-7/DOX^R human breast cancer cells.

Western blot assays were used to analyze MCF-7/DOX^R cell lysates for their contents of important AMPK pathway signaling intermediates, which include ATP citrate lyase (ACLY), glycogen synthase kinase (GSK-3 β), and AMP-activated protein kinase (AMPK α), using β -actin protein levels as the loading control. Treatment with

doxorubicin (for 24 hours at 2 μM) exhibits no effect on phosphorylated and non-phosphorylated ACLY and GSK-3 β levels, in MCF-7/DOX^R cells, when compared with ACLY and GSK-3 β levels in the untreated control (**Fig. 1D**). By contrast, furanodiene treatment (for 24 hours at 50, 100 μM) of these cells significantly induces AMPK phosphorylation, significantly inhibits both ACLY phosphorylation and expression, and significantly inhibits GSK-3 β phosphorylation, in a dose-dependent manner.

3.3. Furanodiene and doxorubicin suppress mitochondrial function and induce phosphorylation of AMPK in doxorubicin-sensitive MCF-7 (MCF-7/DOX^S) human breast cancer cells.

To assess the effect of furanodiene on mitochondrial function in MCF-7/DOXS cells, these cells were treated with furanodiene in increased doses (0, 50, 100 μM) or doxorubicin (2 μM) for four hours. Flow cytometry analysis using MitoTracker[®] Deep Red probe (100 nM) detected and quantitated differences in mitochondrial function between control and treated cells, as shown in **Fig. 2A**. From visual inspection of **Fig. 2A**, mitochondrial function in treated MCF-7/DOX^S cells is suppressed by both furanodiene (dose-dependent) and doxorubicin, when compared to the untreated control (reflected by similar MitoTracker[®] Deep Red MFIs). **Fig. 2B** shows significantly decreased ATP content in both furanodiene- and

doxorubicin-treated cells relative to the untreated controls (measured using an ATP kit). Finally, both furanodiene and doxorubicin were observed to induce phosphorylation of AMPK in these MCF-7/DOX^S cells, as shown in **Fig. 2C**. Collectively, these observations further confirm that the parental MCF-7 line is sensitive to both furanodiene and doxorubicin.

3.4. Furanodiene-induced cell growth inhibition is diminished in presence of the AMPK inhibitor compound C (CC), but elevated in the presence of the AMPK activator AICAR, for MCF-7/DOX^R human breast cancer cells.

MCF-7/DOX^R cells were treated for four hours, either with 2 μ M of compound C (CC), an AMPK inhibitor, or with 50 μ M of AICAR (5-aminoimidazole-4-carboxamide-1- β -4-ribofuranoside, acadesine), an AMPK activator, alone or in combination with 100 μ M of furanodiene. **Figs. 3A** and **3B** show that treatment of MCF-7/DOX^R cells with AMPK inhibitor CC, used alone, enhances mitochondrial function (reflected by an increase in MFI relative to the untreated control), and increases ATP content, as shown in **Fig. 3C**. By contrast, treatment of these cells with the AMPK activator AICAR, used alone, has no significant effect on either mitochondrial function (**Figs. 3A, 3B**) or ATP content (**Fig. 3C**). The growth inhibitory effects of furanodiene, and the effects of CC and AICAR, are also evident by the striking alterations in cell numbers induced by these compounds when viewed

under the microscope. **Fig. 3D** shows that furanodiene treatment (for eight hours at 100 μM) decreases the number of MCF-7/DOX^R cells significantly, in comparison to cells not treated with furanodiene, and that CC treatment (2 μM), which inhibits AMPK, attenuates the reduction in cell number, while AICAR treatment (50 μM) enhances it.

3.5. AMPK activation induced by furanodiene is diminished in presence of CC, but strengthened in the presence of AICAR

AMPK activation induced by furanodiene treatment (for 24 hours at 100 μM) is diminished in the presence of CC, but strengthened in the presence of AICAR in MCF-7/DOX^R cells (**Fig. 3E**). Further evidence pointing to AMPK as the central signaling intermediate is also shown in **Fig. 3E**. The $\gamma\text{-H2A.X}$ biomarker is a reliable immunohistochemical marker for DNA double strand breaks and genomic instability. Furanodiene increases $\gamma\text{-H2A.X}$ expression in these cells, unless they are pre-treated with CC (which decreased furanodiene-induced $\gamma\text{-H2A.X}$ expression) or AICAR (which further enhanced furanodiene-induced $\gamma\text{-H2A.X}$ expression). Of note: in the absence of furanodiene treatment, neither CC nor AICAR treatment of the cells affects expression of $\gamma\text{-H2A.X}$.

3.6. Knockdown of AMPK reverses the effect of furanodiene on mitochondrial

function and metabolic signaling

At the start of this study, Western blotting showed that shAMPK knockdown of AMPK is strong in MCF-7/DOX^R cells. By contrast, knockdown of AMPK expression does not affect HER2 or β -actin expression (**Fig. 4A**), although AMPK-knockdown cells are still resistant to doxorubicin, with an IC₅₀ value of 66.57 μ M (**Fig. 4B**). MCF-7/DOX^R cells transfected with shAMPK are subsequently much less sensitive to furanodiene-induced suppression of ATP content (**Fig. 4C**) and mitochondrial function (**Figs. 5A, B**) than the cells transfected with shControl. In the same cells, however, knockdown of AMPK expression significantly attenuates furanodiene-induced AMPK phosphorylation and γ -H2A.X up-regulation. There is no significant difference in HER2 expression, ACLY phosphorylation, ACLY expression, GSK-3 β phosphorylation, GSK-3 β expression induced by furanodiene in cells transfected with shControl when compared to cells transfected with shAMPK (**Fig. 5C**).

3.7. Knockdown of AMPK attenuates the pro-apoptotic and the growth inhibitory effects of furanodiene

Figs. 5D and **5E** show that knockdown of AMPK expression in MCF-7/DOX^R cells attenuates furanodiene-induced sub-G₁ phase arrest. In addition, measurement of

apoptosis in the cells confirms that knockdown of AMPK expression attenuates the pro-apoptotic effect of furanodiene (**Figs. 6A, 6B**). Finally, knockdown of AMPK expression in the MCF-7/DOX^R cells prevents cell number reductions otherwise induced in these cells by furanodiene (**Fig. 6C**). This effect is confirmed by cell viability comparisons using the MTT assay, as shown in **Fig. 6D**.

4. Discussion and Conclusion

Many *in vitro* and *in vivo* studies have documented the anticancer effects of furanodiene, but none yet have tested the hypothesis that furanodiene-induced anticancer effects are mediated by AMPK^{23,27,36}. In this report, we demonstrate that breast cancer cell chemoresistance to doxorubicin, which can be induced in the well-characterized MCF-7 breast cancer cell line, is still sensitive to furanodiene treatment *via* the AMPK pathway (**Fig. 7**).

Metabolic reprogramming, a mechanism for tumor growth commonly known as the Warburg Effect, and chemoresistance onset in cancer has been studied extensively by others^{37,38}. Our approach applied a more specific working hypothesis, and sought to identify the mechanisms behind restored treatment efficacy in breast cancer cells with induced chemoresistance. The results shown here demonstrate for the first time that furanodiene alters mitochondrial function and intracellular ATP levels, and that it

exerts anticancer effects in induced-MCF-7/DOX^R breast cancer cells via AMPK pathway signaling. Furthermore, we show that this effect of furanodiene affects the levels and functions of important intermediate factors involved in AMPK pathway signaling, include ACLY, GSK-3 β , γ -H2A.X, and HER2.

ACLY is a cytoplasmic enzyme that aids *de novo* fatty acid synthesis by generating acetyl CoA, and its inhibition suppresses tumor cell growth in a subset of cancer types³⁹⁻⁴⁴. Work by others has shown that ACLY depletion induces AMPK phosphorylation, and the phosphorylation levels were found to correlate significantly with levels of oxidative DNA damage *in vitro* and *in vivo*, linking AMPK phosphorylation with cellular ROS levels⁴⁵⁻⁴⁷. **Fig. 1D** provides preliminary evidence that furanodiene may inhibit ACLY.

The GSK-3 β molecule plays dual functional roles in tumorigenesis, acting as a tumor suppressor in some tumor types but promoting the growth and development of others^{48, 49}, and it associates with AMPK- β , the regulatory subunit of AMPK⁵⁰. By showing that furanodiene inhibits GSK-3 β phosphorylation and induces AMPK phosphorylation in **Fig. 1D**, we provide further evidence that furanodiene is an AMPK activator, and that AMPK is tightly linked with ACLY and GSK-3 β pathway intermediates in establishing chemoresistance in tumor cells (**Fig. 5C**).

Other AMPK pathway intermediates have been shown to regulate cell death. AMPK activation is correlated with suppression of HER2 activity, which precedes commitment to cell death⁵¹. Amplification of the gene HER2, and overexpression of its protein, are specific pathological markers in certain human breast cancers, and work is underway in many laboratories toward targeting HER2 for chemotherapy⁵². In our experimental model, we find that HER2 is downregulated by furanodiene, and that this downregulation is still robust even in the presence of CC or AICAR, which down- and up-regulates AMPK activation, respectively (**Fig. 3E**). In addition, we demonstrate that knockdown of AMPK expression fails to reverse furanodiene-induced HER2 regulation (**Fig. 3C**). The results suggest that HER2 might be an upstream factor of AMPK in the anticancer effects of furanodiene (**Fig. 7**).

Still other AMPK pathway intermediates are involved with DNA damage repair. For example, γ -H2A.X is phosphorylated in an AMPK-dependent manner, leading to direct transcriptional and chromatin regulator pathways leading to cellular adaptation to stress⁵³. In **Fig. 3E**, the results show that furanodiene action on γ -H2A.X is involved in its effects on AMPK phosphorylation levels.

Compound C (CC) is a pyrazolopyrimidine derivative that acts as a permeable, reversible and specific AMPK inhibitor, while AICAR is a specific cell-permeable

activator of AMPK. We show here that that AICAR reinforces AMPK activation by furanodiene, and that CC counteracts this effect of furanodiene, by treating MCF-7/DOX^R cells with furanodiene and these other agents, alone or together and assessing the metabolic impact on these cells using various assays of mitochondrial function, ATP content, cell count and AMPK phosphorylation.

During apoptosis, γ -H2A.X phosphorylation is followed by formation of double-strand breaks, and its accumulation in cells often documents and quantitates DNA damage leading to apoptosis⁵⁴⁻⁵⁶. Our results show that γ -H2A.X is upregulated by furanodiene, and that this effect is opposed by CC and shAMPK but assisted by AICAR (**Fig. 3E**). These results confirm that furanodiene inhibits MCF-7 cell growth via increasing cell apoptosis, by way of AMPK, in these cells.

To further confirm that AMPK activation is a direct effect of furanodiene in chemoresistant cancer cells, we transfected MCF-7 cells with shAMPK, to knock down AMPK expression, and then subjected the cells to the aforementioned furanodiene treatment protocol. As expected, our results showed that knockdown of AMPK expression attenuates mitochondrial function suppression, pro-apoptosis, cell growth suppression and cell viability reduction induced by furanodiene. These alterations in mitochondrial function after AMPK knockdown demonstrate that furanodiene (a) inhibits cell growth (**Figs. 6C, 6D**) likely through increasing cell

apoptosis (**Figs. 5D, 5E, 6A, 6B**), and (b) regulates tumor metabolic reprogramming in an AMPK-dependent manner (**Figs. 4C, 5B, 5C**).

Taken together, we show here that furanodiene inhibits cancer cell growth via the AMPK pathway, and causes cell apoptosis via metabolic regulation in chemoresistant MCF-7 breast cancer cells. This is the first investigation of the anticancer potential of furanodiene in chemoresistant cancer cells, and the first investigation to link a relatively new anti-cancer drug, furanodiene, to a relatively old hypothesis for cancer treatment, through targeting tumor metabolism. Finally, this is the first study that links AMPK activation to the effects of furanodiene on cancer cells. We suggest that furanodiene is an anti-cancer agent that may play an important role in addressing the problem of multidrug resistance (and loss of chemotherapeutic efficacy) via intervention in cancer metabolic reprogramming.

In addition, it has been shown that the level of glucose concentration within the tumor microenvironment is a critical variable in cancer response and treatment outcomes. Specifically, only under glucose withdrawal stress was metformin activation of AMPK lethal to breast cancer cells, by circumventing HER2 oncogenic protection of these cells from glucose-deprivation apoptosis⁵⁷. Conversely, high concentrations of glucose (4500 and 9000 mg/L) promote chemoresistance in SGC-7901 gastric cancer cells *in vitro*, and in gastric cancer patients with type 2 diabetes *in vivo*⁵⁸. Of special

interest for future investigation is (a) whether AMPK activation by different stimuli, e.g., glucose starvation (2-deoxyglucose) or metformin, will share similar treatment efficacies to furanodiene-induced AMPK activation in cultured MCF-7/DOX^R breast cancer cells, and (b) where the pathway signals activating AMPK can be integrated within the cell across different stimuli to produce synergistic anticancer effects.

Author contributions

WYT, QWA, and ZZF conceived and organized this study. ZZF designed and conducted all experiments, and revised the manuscript. TW provided data interpretation, and drafted the manuscript. WWQ and VLS revised the manuscript. WCM covered some of the experimental costs. QWA designed some of experiments, provided data interpretation, and revised the manuscript. WYT supported and supervised the study. All authors read and approved the manuscript.

Conflicts of interests

The authors declared that they have no competing interests.

Abbreviations

AMPK (AMP-activated protein kinase); ATP (Adenosine-5'-triphosphate); ACLY (ATP-Citrate Lyase); GSK-3 β (Glycogen synthase kinase-3 β); MDR (Multidrug resistance); ADP (Adenosine diphosphate); NADPH (Nicotinamide adenine dinucleotide phosphate); FH (fumarate hydratase); HIF α (hypoxia-inducible factor α); LDHA (Lactate dehydrogenase A); Nampt (Nicotinamide phosphoribosyltransferase); TPA (12-O-tetradecanoylphorbol-13-acetate); ER (Estrogen receptor); PPAR γ (peroxisome proliferator-activated receptor γ); FUR (Furanodiene); DOX (Doxorubicin); FBS (Fetal bovine serum); PBS (Phosphate-buffered saline); PS (Penicillin-streptomycin); EDTA (Ethylenediaminetetraacetic acid); MTT (3-[4,5-Dimethyl-2-thiazolyl]-2,5-diphenyltetrazolium bromide); PI (Propidium iodide); RIPA (Radioimmunoprecipitation assay); SDS-PAGE (Sodium dodecyl sulphate-Polyacrylamide gel electrophoresis); PVDF (Polyvinylidene fluoride); CC (Compound C); AICAR (5-aminoimidazole-4-carboxamide-1- β -D-ribofuranoside, adenosine)

Acknowledgments

This study was supported by the Macao Science and Technology Development Fund (077/2011/A3 and 048/2013/A2), and the Research Fund of University of Macau (CPG2014-00012-ICMS, UL016/09Y4/CMS/WYT01/ICMS and MYRG208 (Y3-L4)-ICMS11-WYT). W.A. Qiang was supported by the Baskes Foundation and

the Robert H. Lurie Comprehensive Cancer Center at Northwestern University. We thank Stacy Ann Kujawa at Northwestern University's Feinberg School of Medicine for her critical proofreading of the manuscript. We also thank Sheng-Peng Wang and An-Qi Wang prepared for the cell lines.

References

1. A.-M. Florea and D. Busselberg, *J Local Glob Health Sci*, 2013, DOI: 10.5339/jlghs.2013.1.
2. D. C. Wallace, *Cold Spring Harb Symp Quant Biol*, 2005, **70**, 363-374.
3. S. Ruetz and P. Gros, *Trends Pharmacol Sci*, 1994, **15**, 260-263.
4. B. Bhattacharya, M. F. Mohd Omar and R. Soong, *Br J Pharmacol*, 2016, DOI: 10.1111/bph.13422.
5. D. G. Hardie, *Clin Cancer Res*, 2015, DOI: 10.1158/1078-0432.
6. M. Saxena, M. A. Stephens, H. Pathak and A. Rangarajan, *Cell death & disease*, 2011, **2**, e179.
7. J. P. Gillet, T. Efferth, D. Steinbach, J. Hamels, F. de Longueville, V. Bertholet and J. Remacle, *Cancer Res*, 2004, **64**, 8987-8993.
8. J. R. Fay, V. Steele and J. A. Crowell, *Cancer Prev Res (Phila)*, 2009, **2**, 301-309.
9. D. G. Hardie, *Nat Rev*, 2007, **8**, 774-785.

10. S. Fogarty and D. G. Hardie, *Biochimica et biophysica acta*, 2010, **1804**, 581-591.
11. F. P. Kuhajda, *Int J Obes (Lond)*, 2008, **32 Suppl 4**, S36-41.
12. D. G. Hardie, *Biochem Soc Trans*, 2011, **39**, 1-13.
13. D. G. Hardie, *Diabetes*, 2013, **62**, 2164-2172.
14. B. Faubert, G. Boily, S. Izreig, T. Griss, B. Samborska, Z. Dong, F. Dupuy, C. Chambers, B. J. Fuerth, B. Viollet, O. A. Mamer, D. Avizonis, R. J. DeBerardinis, P. M. Siegel and R. G. Jones, *Cell Metab*, 2013, **17**, 113-124.
15. G. Zadra, J. L. Batista and M. Loda, *Mol Cancer Res*, 2015, **13**, 1059-1072.
16. I. Dando, M. Donadelli, C. Costanzo, E. Dalla Pozza, A. D'Alessandro, L. Zolla and M. Palmieri, *Cell Death Dis*, 2013, **4**, e664.
17. S. M. Jeon, N. S. Chandel and N. Hay, *Nature*, 2012, **485**, 661-665.
18. W. H. Tong, C. Sourbier, G. Kovtunovych, S. Y. Jeong, M. Vira, M. Ghosh, V. Romero, R. Sougrat, S. Vaulont, B. Viollet, Y. S. Kim, S. Lee, J. Trepel, R. Srinivasan, G. Bratslavsky, Y. Yang, W. M. Linehan and T. A. Rouault, *Cancer cell*, 2011, **20**, 315-327.
19. J. Zhou, W. Huang, R. Tao, S. Ibaragi, F. Lan, Y. Ido, X. Wu, Y. O. Alekseyev, M. E. Lenburg, G. F. Hu and Z. Luo, *Oncogene*, 2009, **28**, 1993-2002.
20. K. H. Lee, E. C. Hsu, J. H. Guh, H. C. Yang, D. Wang, S. K. Kulp, C. L. Shapiro and C. S. Chen, *J Biol Chem*, 2011, **286**, 39247-39258.
21. C. Qu, W. Zhang, G. Zheng, Z. Zhang, J. Yin and Z. He, *Mol Cell Biochem*,

- 2014, **386**, 63-71.
22. D. Rui, C. Xiaoyan, W. Taixiang and L. Guanjian, *Cochrane Database Syst Rev*, 2007, DOI: 10.1002/14651858.CD006054.
 23. Z. Zhong, Y. Dang, X. Yuan, W. Guo, Y. Li, W. Tan, J. Cui, J. Lu, Q. Zhang, X. Chen and Y. Wang, *Cell Physiol Biochem*, 2012, **30**, 778-790.
 24. Y. Xiao, F. Q. Yang, S. P. Li, J. L. Gao, G. Hu, S. C. Lao, E. L. Conceicao, K. P. Fung, Y. T. Wangl and S. M. Lee, *Cancer Biol Ther*, 2007, **6**, 1044-1050.
 25. E. Ma, X. Wang, Y. Li, X. Sun, W. Tai, T. Li and T. Guo, *Cancer Lett*, 2008, **271**, 158-166.
 26. X. Chen, L. Pei, Z. Zhong, J. Guo, Q. Zhang and Y. Wang, *Phytomedicine*, 2011, **18**, 1238-1243.
 27. W. S. Xu, Y. Y. Dang, J. J. Guo, G. S. Wu, J. J. Lu, X. P. Chen and Y. T. Wang, *Evid Based Complement Alternat Med*, **2012**, 426521.
 28. Q. Kong, F. Sun and X. Chen, *Cell J*, 2013, **15**, 160-165.
 29. W. S. Xu, T. Li, G. S. Wu, Y. Y. Dang, W. H. Hao, X. P. Chen, J. J. Lu and Y. T. Wang, *Am J Chin Med*, 2014, **42**, 243-255.
 30. W. S. Xu, Y. Y. Dang, X. P. Chen, J. J. Lu and Y. T. Wang, *Phytother Res*, 2014, **28**, 296-299.
 31. Z. F. Zhong, Y. B. Li, S. P. Wang, W. Tan, X. P. Chen, M. W. Chen and Y. T. Wang, *J Cell Biochem*, 2012, **113**, 2643-2651.
 32. Z. Zhong, W. Tan, X. Chen and Y. Wang, *Eur J Pharmacol*, 2014, **737**, 1-10.

33. S. Ai, T. Jia, W. Ai, J. Duan, Y. Liu, J. Chen, X. Liu, F. Yang, Y. Tian and Z. Huang, *Br J Pharmacol*, 2013, **168**, 1719-1735.
34. Q. Y. Chen, D. M. Jiao, L. F. Wang, L. Wang, H. Z. Hu, J. Song, J. Yan, L. J. Wu and J. G. Shi, *Mol Biosyst*, 2015, **11**, 859-868.
35. Z. Zhong, L. J. Liu, Z. Q. Dong, L. Lu, M. Wang, C. H. Leung, D. L. Ma and Y. Wang, *Chem Commun (Camb)*, 2015, **51**, 11178-11181.
36. Z. F. Zhong, W. A. Qiang, C. M. Wang, W. Tan and Y. T. Wang, *Eur J Pharmacol*, 2016, **774**, 10-19.
37. V. Poli and A. Camporeale, *Front Oncol*, 2015, **5**, 121.
38. S. H. Wu, J. F. Bi, T. Cloughesy, W. K. Cavenee and P. S. Mischel, *Cancer Biol Med*, 2014, **11**, 255-263.
39. M. E. Beckner, W. Fellows-Mayle, Z. Zhang, N. R. Agostino, J. A. Kant, B. W. Day and I. F. Pollack, *Int J Cancer*, 2010, **126**, 2282-2295.
40. J. I. Hanai, N. Doro, P. Seth and V. P. Sukhatme, *Cell death & disease*, 2013, **4**, e696.
41. M. Chypre, N. Zaidi and K. Smans, *Biochem Biophys Res Commun*, 2012, **422**, 1-4.
42. N. Zaidi, J. V. Swinnen and K. Smans, *Cancer research*, 2012, **72**, 3709-3714.
43. X. Y. Zu, Q. H. Zhang, J. H. Liu, R. X. Cao, J. Zhong, G. H. Yi, Z. H. Quan and G. Pizzorno, *Recent Pat Anticancer Drug Discov*, 2012, **7**, 154-167.
44. A. D. Khwairakpam, M. S. Shyamananda, B. L. Sailo, S. R. Rathnakaram, G.

- Padmavathi, J. Kotoky and A. B. Kunnumakkara, *Curr Drug Targets*, 2015, **16**, 156-163.
45. H. N. Lemus and C. O. Mendivil, *J Clin Lipidol*, 2015, **9**, 384-389.
46. S. L. Pinkosky, S. Filippov, R. A. Srivastava, J. C. Hanselman, C. D. Bradshaw, T. R. Hurley, C. T. Cramer, M. A. Spahr, A. F. Brant, J. L. Houghton, C. Baker, M. Naples, K. Adeli and R. S. Newton, *J Lipid Res*, 2013, **54**, 134-151.
47. T. Migita, S. Okabe, K. Ikeda, S. Igarashi, S. Sugawara, A. Tomida, R. Taguchi, T. Soga and H. Seimiya, *Am J Pathol*, 2013, **182**, 1800-1810.
48. J. Luo, *Cancer Lett*, 2009, **273**, 194-200.
49. K. Miyashita, M. Nakada, A. Shakoori, Y. Ishigaki, T. Shimasaki, Y. Motoo, K. Kawakami and T. Minamoto, *Anticancer Agents Med Chem*, 2009, **9**, 1114-1122.
50. T. Suzuki, D. Bridges, D. Nakada, G. Skiniotis, S. J. Morrison, J. D. Lin, A. R. Saltiel and K. Inoki, *Molecular cell*, 2013, **50**, 407-419.
51. T. Z. Jhaveri, J. Woo, X. Shang, B. H. Park and E. Gabrielson, *Oncotarget*, 2015, **6**, 14754-14765.
52. R. Dittadi and M. Gion, *J Natl Cancer Inst*, 2000, **92**, 1443-1444.
53. D. Bungard, B. J. Fuerth, P. Y. Zeng, B. Faubert, N. L. Maas, B. Viollet, D. Carling, C. B. Thompson, R. G. Jones and S. L. Berger, *Science*, 2010, **329**, 1201-1205.

54. L. J. Kuo and L. X. Yang, *In Vivo*, 2008, **22**, 305-309.
55. A. Kinner, W. Wu, C. Staudt and G. Iliakis, *Nucleic Acids Res*, 2008, **36**, 5678-5694.
56. E. P. Rogakou, D. R. Pilch, A. H. Orr, V. S. Ivanova and W. M. Bonner, *J Biol Chem*, 1998, **273**, 5858-5868.
57. J. A. Menendez, C. Oliveras-Ferraros, S. Cufi, B. Corominas-Faja, J. Joven, B. Martin-Castillo and A. Vazquez-Martin, *Cell cycle*, 2012, **11**, 2782-2792.
58. W. Zhao, R. Chen, M. Zhao, L. Li, L. Fan and X. M. Che, *Mol Med Rep*, 2015, **12**, 843-850.

Figure Legends

Fig. 1. Effects of furanodiene (FUR or F) on mitochondrial function in doxorubicin-resistant MCF-7 (MCF-7/DOX^R) human breast cancer cells. MCF-7/DOX^R cells were treated with furanodiene in increased doses (0, 50, 100 μ M) or with doxorubicin (2 μ M). (A) Mitochondrial functions of these MCF-7/DOX^R cells were assessed after four hours by means of the mean fluorescence intensity (MFI) obtained *via* flow cytometry analysis (100 nM MitoTracker[®] Deep Red probe, incubated for 15 min). (B) MFIs of cells treatment groups were normalized to and compared with the MFI of untreated control. (C) ATP content was quantitated using an ATP kit following the manufacturer's protocol. Fluorescence intensities were

determined using 500 μg loading protein, and was normalized to and compared with the fluorescence intensity of the untreated control. (D) Cell lysates were analyzed for their contents of phosphorylated and expression levels of ATP citrate lyase (ACLY), glycogen synthase kinase (GSK-3 β), and AMP-activated protein kinase (AMPK α) using Western blot assay, with β -actin protein levels serving as the loading control. Data represent the mean \pm S.E.M of three independent experiments. * $P < 0.05$, ** $P < 0.01$ and *** $P < 0.001$.

Fig. 2. Effects of furanodiene (FUR or F) on mitochondrial function in doxorubicin-sensitive MCF-7 (MCF-7/DOX^S) human breast cancer cells.

MCF-7/DOX^S cells were treated with furanodiene in increased doses (0, 50, 100 μM) or with doxorubicin (2 μM). (A) Mitochondrial functions of these MCF-7/DOX^S cells were assessed after four hours by means of the mean fluorescence intensity (MFI) obtained *via* flow cytometry analysis (100 nM MitoTracker[®] Deep Red probe, incubated for 15 min). (B) ATP content was quantitated using an ATP kit following the manufacturer's protocol. Fluorescence intensities were determined using 500 μg loading protein, and was normalized to and compared with the fluorescence intensity of the untreated control. (C) Cell lysates were analyzed for their contents of phosphorylated and expression levels of AMP-activated protein kinase (AMPK α) using Western blot assay, with β -actin protein levels serving as the loading control. Data represent the mean \pm S.E.M of three independent experiments. * $P < 0.05$ and

*** $P < 0.001$.

Fig. 3. Effects of an AMPK inhibitor or activator and furanodiene (FUR or F) on mitochondrial function in doxorubicin-resistant MCF-7 (MCF-7/DOX^R) human breast cancer cells. MCF-7/DOX^R cells were pro-treated with either 2 μ M of compound C (CC), an AMPK inhibitor, or with 50 μ M of AICAR (AI), an AMPK activator, then treated with 100 μ M of furanodiene. (A) Mitochondrial functions of these MCF-7/DOX^R cells were assessed after four hours by means of the mean fluorescence intensity (MFI) obtained *via* flow cytometry analysis (100 nM MitoTracker® Deep Red probe, incubated for 15 min). (B) MFIs of cells treatment groups were normalized to and compared with those of their respective controls. (C) ATP content was quantitated using an ATP kit following the manufacturer's protocol. Fluorescence intensities of treatment groups was normalized to and compared with the fluorescence intensity of the untreated control. (D) Cell density was observed with a light microscope under a 100 \times magnification and counted. All mean cell numbers were normalized to the cell numbers in the field of view of the untreated control. (E) Cell lysates were analyzed for their contents of human epidermal growth factor receptor (HER2), phosphorylated AMP-activated protein kinase (p-AMPK α), and a histone protein (γ -H2A.X) using Western blot assay, with GAPDH protein levels serving as the loading control. Data represent the mean \pm S.E.M of three independent experiments. * $P < 0.05$ and ** $P < 0.01$.

Fig. 4. Effects of furanodiene (FUR) on mitochondrial function alterations in AMPK-knockdown, doxorubicin-resistant MCF-7 (MCF-7/DOX^R) human breast cancer cells.

MCF-7/DOX^R cells were transfected with shRNA using Lipofectamine 2000 for four hours, returned to culture for 48 hours. (A) Cell lysates from non-transfected, transfected shControl, and AMPK-knockdown MCF-7/DOX^R cells were harvested and analyzed for their contents of AMPK α and HER2 using Western blot assay to confirm the specificity and effectiveness the shRNA transfection procedure, with β -actin protein levels serving as the loading control. (B) Non-transfected, transfected shControl, and AMPK-knockdown MCF-7/DOX^R cells were seeded in 96-well plates at a density of 10,000/well, and then were treated with doxorubicin for 24 hours. Cell viability was determined *via* MTT assay. (C) The ATP content of transfected shControl and AMPK-knockdown MCF-7/DOX^R cells treated for four hours with furanodiene (100 μ M) was quantitated using an ATP kit following the manufacturer's protocol. Fluorescence intensities of treatment groups were normalized to and compared with the fluorescence intensity of untreated transfected shControl cells. Data represent the mean \pm S.E.M of three independent experiments. * $P < 0.05$.

Fig. 5. AMPK is a central mediator of furanodiene (FUR) anticancer effects in the mitochondria of doxorubicin-resistant MCF-7 (MCF-7/DOX^R) human breast

cancer cells.

MCF-7/DOX^R cells were transfected with shRNA using Lipofectamine 2000 for four hours, returned to culture for 48 hours, and then treated with furanodiene (100 μ M). (A) Mitochondrial functions of these MCF-7/DOX^R cells were assessed after four hours by means of the mean fluorescence intensity (MFI) obtained *via* flow cytometry analysis (100 nM MitoTracker® Deep Red probe, incubated for 15 min). (B) The MFI of AMPK-knockdown cells were compared with the MFI of the transfected shControl cells. (C) Cell lysates were analyzed for their contents of phosphorylated and expression levels of ATP citrate lyase (ACLY), glycogen synthase kinase (GSK-3 β), and AMP-activated protein kinase (AMPK α) using Western blot assay. Human epidermal growth factor receptor (HER2) and histone protein (γ -H2A.X) were also analyzed. GAPDH protein levels served as the loading control. (D) Cell cycle distributions were determined after 24-hour furanodiene treatment using flow cytometry analysis of cell DNA content (stained with propidium iodide). (E) The percentages of sub-G1 phase cells (out of total cells) were determined for each of the transfected shControl and AMPK-knockdown experiment conditions, and then these were compared statistically. Data expressed as mean \pm S.E.M of three independent experiments. ** $P < 0.01$.

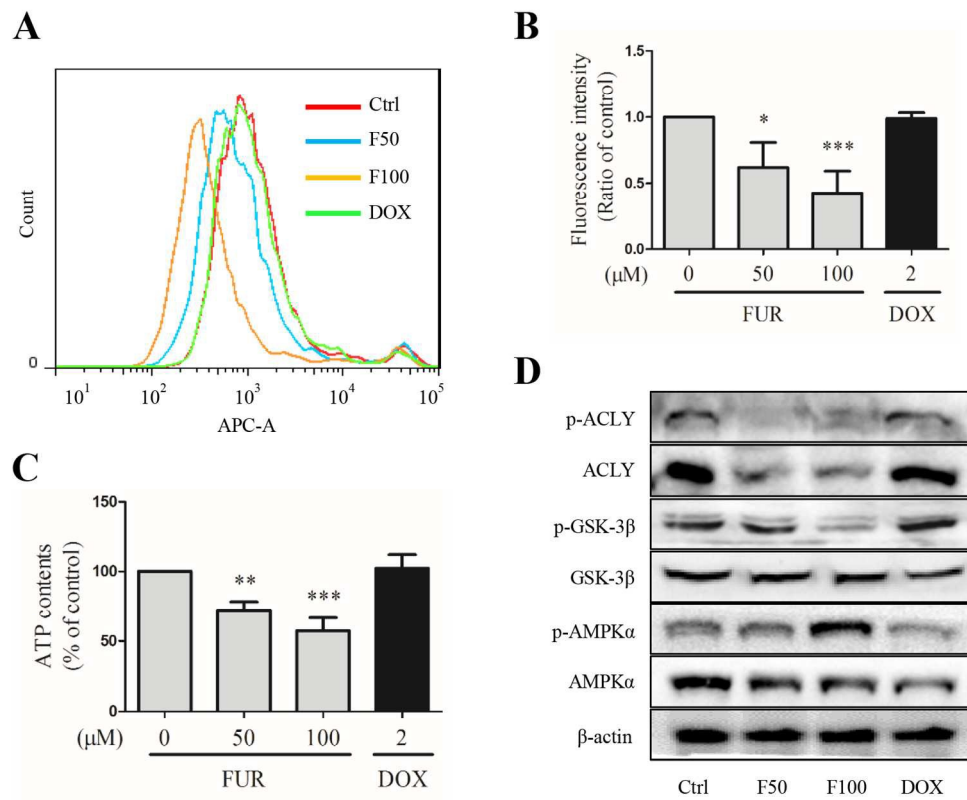
Fig. 6. Furanodiene (FUR)-induced cell apoptosis occurs *via* AMPK signaling in doxorubicin-resistant MCF-7 (MCF-7/DOX^R) human breast cancer cells.

MCF-7/DOX^R cells were transfected with shRNA using Lipofectamine 2000 for four hours, returned to culture for 48 hours, and then treated with furanodiene (100 μ M). (A) Cells were probed with Annexin V (FITC-A) and PI (PE-A) dyes, and then analyzed by flow cytometry. (B) The percentages of late-stage apoptotic cells (Annexin V and PI double-positive cells, Q2) and early-stage apoptotic cells (Annexin V and PI double-positive cells, Q3) were calculated, and then these were compared statistically. (C) Cell density was observed with a light microscope under a 400 \times magnification. (D) Cells were seeded in 96-well plates at a density of 10,000/well, and cell viability was determined *via* MTT assay. Data represent the mean \pm S.E.M of three independent experiments. * $P < 0.05$.

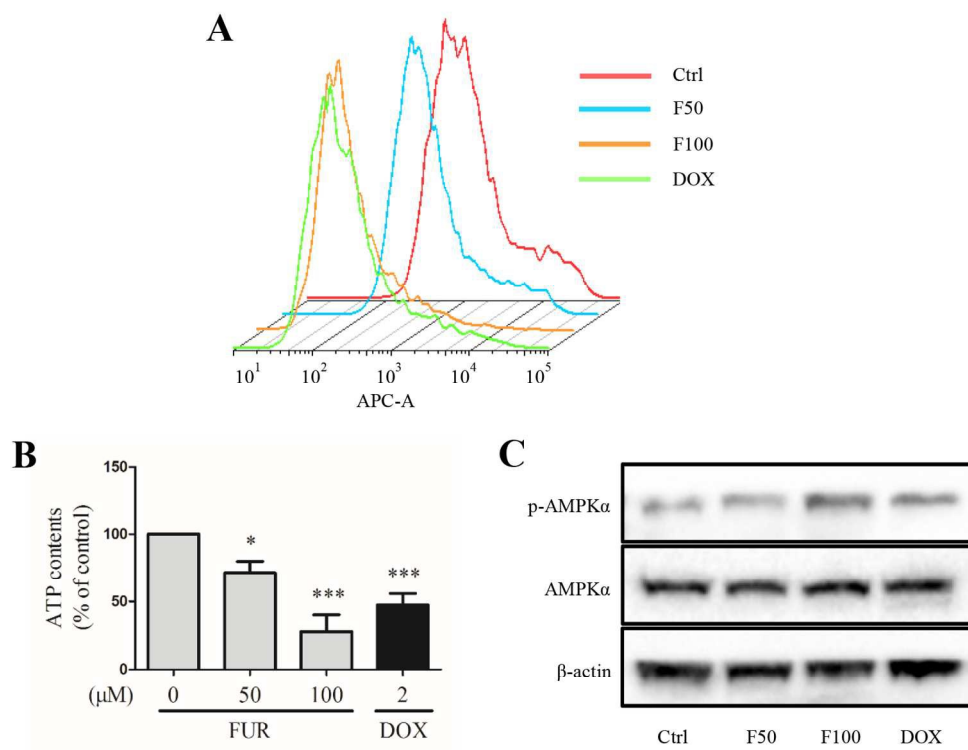
Fig. 7. Furanodiene (FUR)-induced anticancer mechanism and doxorubicin-resistant MCF-7 (MCF-7/DOX^R) breast cancer cell outcomes.

AMPK is an important energy-sensing enzyme regulating many aspects of metabolic reprogramming. Evidence exists that targeting AMPK may exert anti-Warburg and anti-proliferative effects by enhancing mitochondrial oxidation and biogenesis. Using the AMPK inhibitor compound C (CC), the AMPK gene silencer shAMPK, and the AMPK activator AICAR, we demonstrated that the AMPK pathway is the essential mechanism by which furanodiene induces its anticancer effect in MCF-7/DOX^R breast cancer cells. Important AMPK signaling pathway intermediates, including ATP citrate lyase (ACLY) and glycogen synthase kinase (GSK-3 β), are also inhibited by

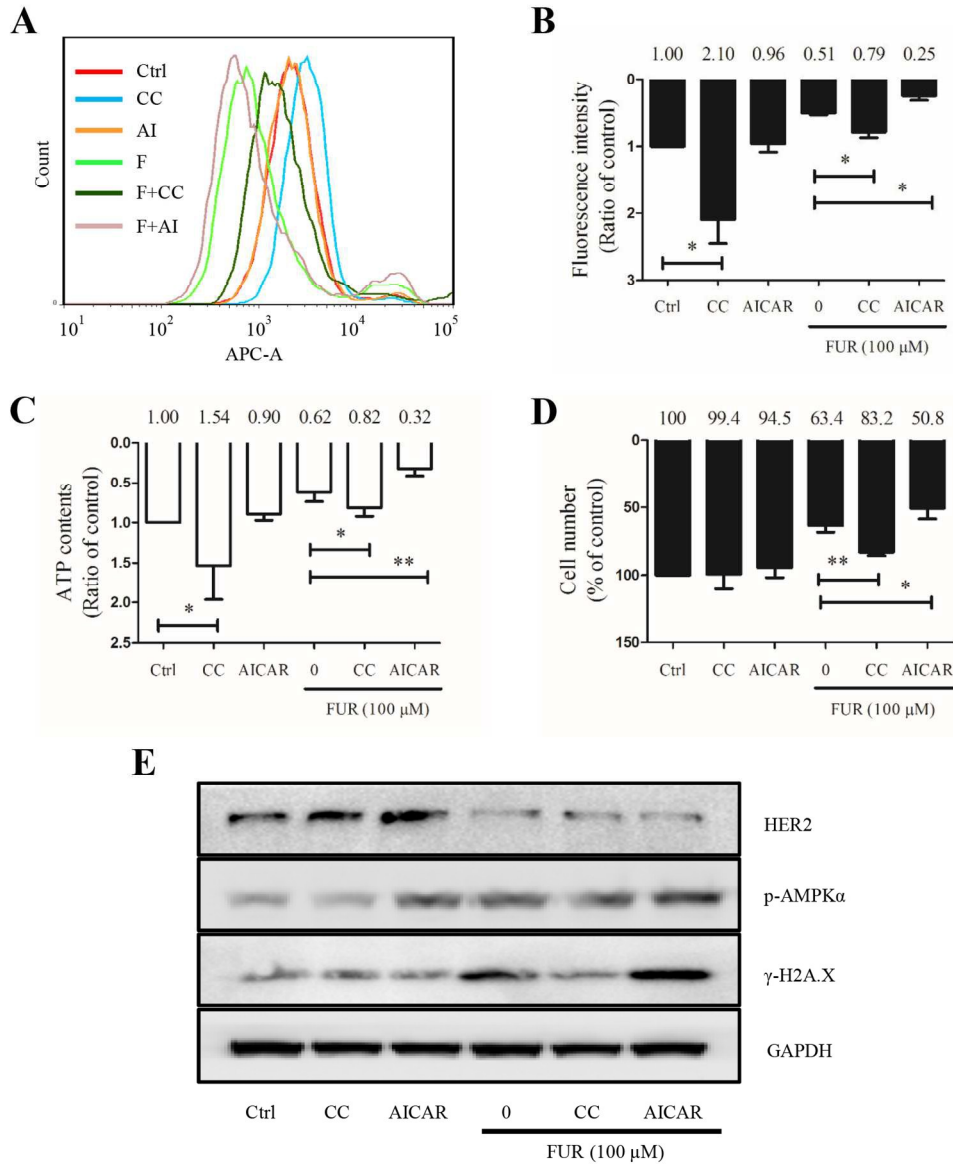
furanodiene; whether by AMPK direct involvement has yet to be seen. Furanodiene is also responsible for the robust downregulation of HER2 documented in these studies, even in the presence of CC and AICAR. This is important because HER2 is a pathological marker specific to some aggressive human breast cancers. This preliminary evidence suggests that HER2 is an upstream factor that governs AMPK activation in furanodiene-mediated anticancer activity.



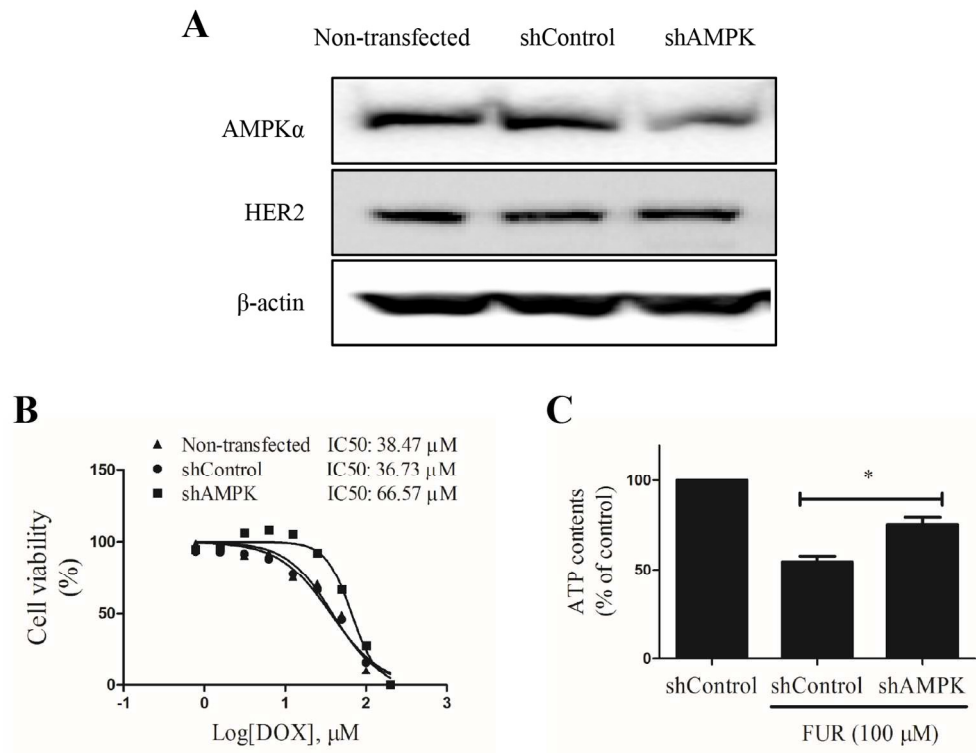
144x120mm (300 x 300 DPI)



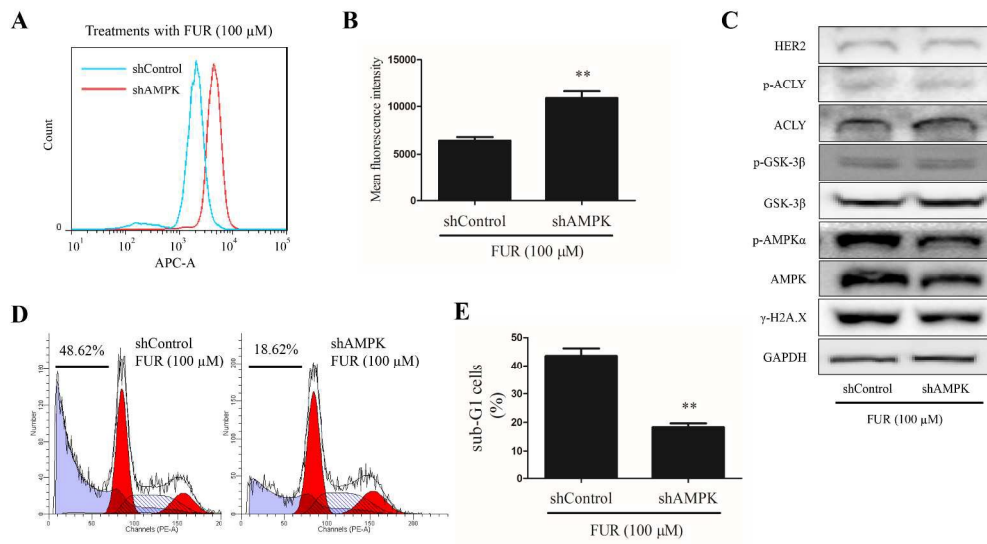
144x112mm (300 x 300 DPI)



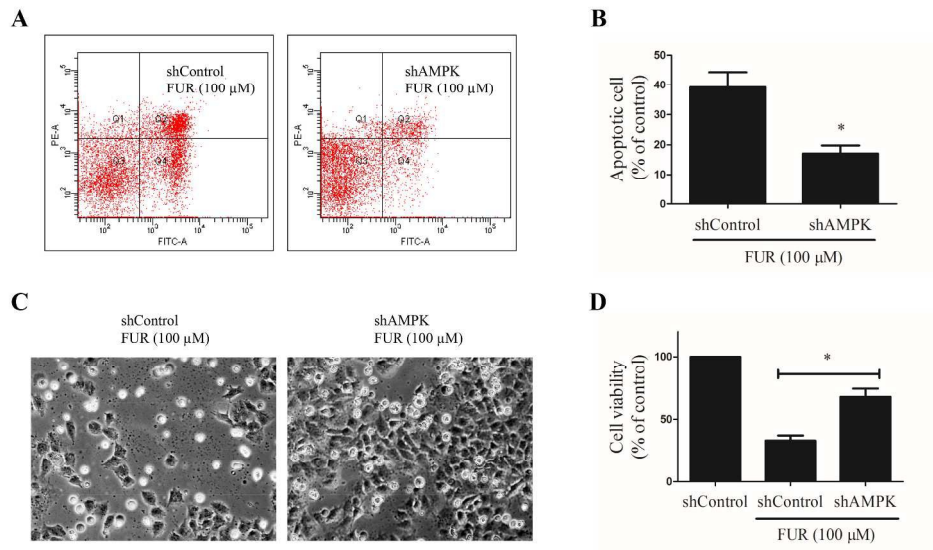
144x175mm (300 x 300 DPI)



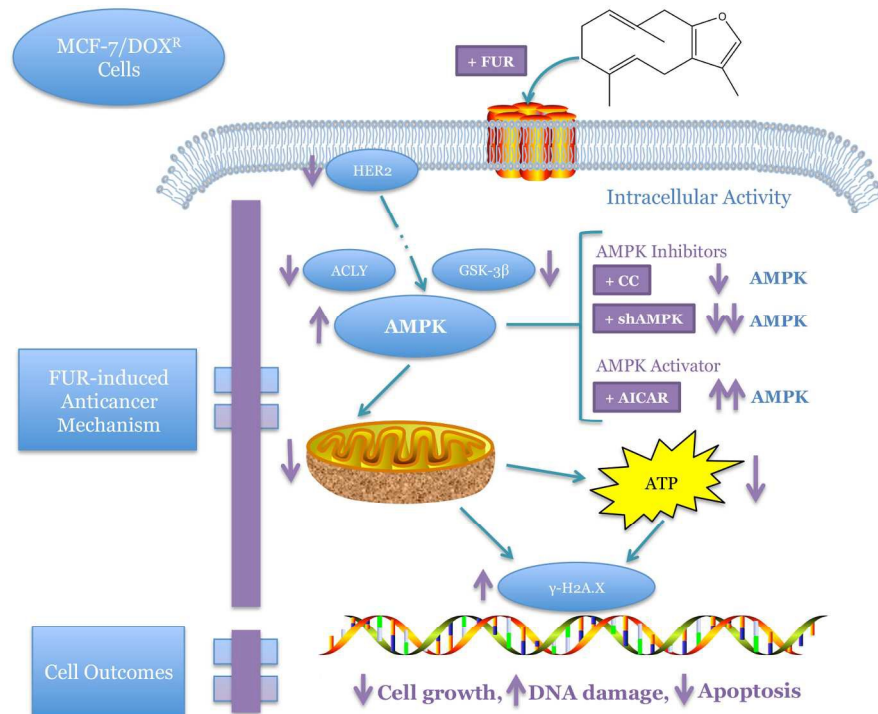
145x113mm (300 x 300 DPI)



296x166mm (300 x 300 DPI)



296x166mm (300 x 300 DPI)



175x127mm (300 x 300 DPI)